Tellus (1981), *33*, 488–504

Non-linear internal waves in shallow water. A theoretical and experimental study

By M. A. HELAL* and J. M. MOLINES, *Institut de Mécanique de Grenoble, B.P. 53 X—38041 Grenoble Cedex, France*

(Manuscript received July 22, in final form November 21, 1980

ABSTRACT

A study of non-linear internal waves is introduced with the shallow water theory, in two layers of perfect fluids. After the establishment of a general differential system, the particular case of progressive waves and standing waves is more completely studied and the development leads to a Boussinesq equation for the first-order term. A solution is found as a cnoidal wave in both cases. Laboratory experiments are carried out to test the analytical solution on a standing internal wave and show that even for highly non-linear internal waves our first-order solution describes the wave shape with an accuracy better than 5%.

1. Introduction

1.1. *The problem*

Since Boussinesq (1871), Rayleigh (1883) and Korteweg and de Vries (1895), a considerable amount of work has been done on non-linear waves. Free surface waves, both cnoidal (periodic) and solitary, have been studied. (See, for instance, Whitham (1974) for bibliography.) Keulegan (1953) and Long (1956) did the initial work on internal waves. They applied Boussinesq's and Rayleigh's free surface wave theories, respectively, to internal waves. After that, most work has been devoted to solitary waves. Studies of internal solitary waves have been pursued by numerous authors from various points of view. Peters and Stoker (1960) carried out an original study of internal solitary waves in both two-layer fluid and a fluid with a continuous stratification. Later, Benjamin (1967) and Davis and Acrivos (1967) did similar work, but for fluids having a lower layer of infinite depth. Somewhat earlier, Ter-Krikorov (1962) and Yanovitch (1962) presented a fundamental mathematical confirmation of the expansion used in this type of theory. The work of Thorpe (1968) allowed very good visualization of both linear and non-linear internal waves. Later, more specific studies were done on internal solitary waves, for instance Grimshaw (1972, 1978) who studied the evolution of such a wave propagating in a channel of arbitrary cross section. Yamasaki and Kakutani (1978), Benney and Ko (1978) and Miles (1979) dealt with the problem of cubic non-linearity.

In parallel, Lee and Beardsley (1974), Maxworthy (1979) and Djordjevic and Redekopp (1978) discussed the generation and fission of internal solitary waves connected with bottom topography. Some of the observations of non-linear internal waves, like those of Hunkins and Fliegel (1973), Apel et al. (1975) and Farmer (1978), can be interpreted by means of the latter theories. Lee and Beardsley (1974) and Maxworthy (1976) also carried out some laboratory experiments which confirmed their work.

Although this review is not comprehensive, it is clear that all these investigations are limited to studies of solitary internal waves which propagate to the right only. This precludes the case of non-linear internal standing waves. The aim of this paper is to study the problem of non-linear internal standing waves, which propagate at the interface of a two-layer, immiscible, incompressible perfect fluid, in a two-dimensional rectangular tank. The flow is assumed to be irrotational. We also present the results of laboratory experiments which were carried out to verify the mathematical results.

* Permanent address: Department of Mathematics, Cairo University, Egypt.

0040-2826/81/040488-17$02.50/0

1.2. *Notation*

The following notations are used in the text:

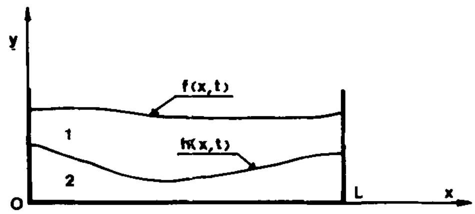

Fig. 1. Notations used in the text.

The coordinate system is defined in Fig. 1.

L = length of the tank.
H_1, H_2 = thickness at rest of the upper and lower layer, respectively.
ρ_1, ρ_2 = constant density of the upper and lower layer, respectively.
P_1, P_2 = pressure of the upper and the lower layer, respectively.
u, v = horizontal and vertical components of the velocity, respectively. (The index on each component defines the layer: 1 for the upper layer, 2 for the lower layer.)
$y = f(x, t)$ = free surface equation, f being one of the unknown functions of our problem.
$y = h(x, t)$ = interface equation and determination of the interfacial position is the final aim of the theoretical part.

2. Basic equations

2.1. *Hydrodynamic equation*

Since we have made the assumption of an irrotational flow, we introduce $\varphi^{(i)}$ $(i = 1, 2)$ which is the velocity potential, i.e. $u^{(i)} = \varphi_x^{(i)}$ $v^{(i)} = \varphi_y^{(i)}$. The basic equations can be written (e.g. Kakutani et al., 1978):

the dynamic equation

$$\vec{\nabla}\left(\varphi_t^{(i)} + \tfrac{1}{2}(\varphi_x^{(i)^2} + \varphi_y^{(i)^2}) + gy + \frac{p^{(i)}}{\rho_i}\right) = 0 \quad (i = 1, 2) \tag{1}$$

the continuity equation

$$\nabla^2 \varphi^{(i)} = 0 \tag{2}$$

Equation (1) gives immediately

$$\frac{p^{(i)}}{\rho_i} = -\{\varphi_t^{(i)} + \tfrac{1}{2}(\varphi_x^{(i)^2} + \varphi_y^{(i)^2}) + gy + C^{(i)}(t)\} \quad (i = 1, 2) \tag{3}$$

where $C^{(i)}$ is an arbitrary function of t, and will be fixed by boundary conditions later.

2.2. *Boundary conditions*

We assume that all the boundaries of the domain are impermeable, including the free surface and the interface. For the latter two, we also impose a pressure condition.

(*a*) At the ends

$$\varphi_x^{(i)} = 0 \quad \text{for } x = 0, L \text{ and } (i = 1, 2) \tag{4}$$

(*b*) At the bottom

$$\varphi_y^{(2)} = 0 \quad \text{for } y = 0 \tag{5}$$

(*c*) On the free surface

$$\varphi_y^{(1)} = f_x \varphi_x^{(1)} + f_t \quad \text{for } y = f(x, t) \tag{6}$$

The pressure is assumed to be constant and equal to zero. Then from eq. (3),

$$\varphi_t^{(1)} + \tfrac{1}{2}(\varphi_x^{(1)^2} + \varphi_y^{(1)^2}) + gf + C^{(1)}(t) = 0 \quad \text{for } y = f(x, t) \tag{7}$$

$C^{(1)}(t)$ can be determined from the solution at rest: $C^{(1)} = -g(H_1 + H_2)$.

(*d*) On the interface

$$\varphi_y^{(i)} = h_x \varphi_x^{(i)} + h_t \quad \text{for } y = h(x, t) \quad (i = 1, 2) \tag{8}$$

And since the fluid is perfect we ignore surface tension for $y = h(x, t)$, $p_1 = p_2$. From (3) we have

$$\rho_1\{\varphi_t^{(1)} + \tfrac{1}{2}(\varphi_x^{(1)^2} + \varphi_y^{(1)^2}) + gh + C^{(1)}\} = \rho_2\{\varphi_t^{(2)} + \tfrac{1}{2}(\varphi_x^{(2)^2} + \varphi_y^{(2)^2}) + gh + C^{(2)}\} \quad \text{for } y = h(x, t) \tag{9}$$

$C^{(2)}$ can also be determined from the solution at rest: $C^{(2)} = -g(\rho_1 H_1 + \rho_2 H_2)$.

3. The shallow water theory

3.1. *Coordinate stretching and expansion*

In this type of problem, the horizontal dimensions are much greater than the vertical dimensions. We introduce the coordinate stretching defined as:

$$\bar{X} = \varepsilon x; \quad \bar{Y} = y; \quad \tau = \varepsilon t \tag{10}$$

where ε is a small but unknown parameter. We expand the dependent variables around the undisturbed uniform state as an asymptotic series of the same parameter.

$$\varphi^{(i)} = \sum_{n=0}^{\infty} \varepsilon^{2n+1} \varphi_{2n+1}^{(i)}(\bar{X}, \bar{Y}, \tau)$$

$$f = \sum_{n=0}^{\infty} \varepsilon^{2n} f_{2n}(\bar{X}, \bar{Y}, \tau)$$

$$h = \sum_{n=0}^{\infty} \varepsilon^{2n} h_{2n}(\bar{X}, \bar{Y}, \tau). \tag{11}$$

with

$$\varphi_0 \equiv 0; \quad f_0 = H_1 + H_2; \quad h_0 = H_2.$$

The boundary conditions on the free surface and on the interface are expanded with a Taylor expansion of the type:

$$[H]_{y=y_0+\varepsilon A} = [H]_{y_0} + \varepsilon A[H_y]_{y_0} + \frac{(\varepsilon A)^2}{2!}[H_{yy}]_{y_0} + \frac{(\varepsilon A)^3}{3!}[H_{yyy}]_{y_0} + \cdots \tag{12}$$

Introducing (10) and (11) using the expansion (12) in eqs. (1)–(9), we can apply the standard procedure of this method to obtain an ordered set of equations to be solved.

4. Orders of approximations

4.1. *First-order approximation*

$$\varphi^{(i)}_{1\bar{Y}\bar{Y}} = 0 \quad (i = 1, 2)$$

$$\varphi^{(1)}_{1\bar{Y}} = 0 \quad \text{for } \bar{Y} = H_1 + H_2; \quad \varphi^{(i)}_{\bar{Y}} = 0 \quad \text{for } \bar{Y} = H_2; \quad \varphi^{(2)}_{y} = 0 \quad \text{for } \bar{Y} = 0 \tag{13}$$

which finally gives:

$$\varphi^{(i)}_1 = B^{(i)}(\bar{X}, \tau) \quad (i = 1, 2) \tag{14}$$

and

$$B^{(i)}_{\bar{X}} = 0 \quad \text{for } \bar{X} = 0 \quad \text{and} \quad \bar{X} = \varepsilon L = l \tag{15}$$

4.2. *The second-order approximation*

From eqs. (7) and (9) we have the following relations:

$$f_2(\bar{X}, \tau) = -\frac{1}{g}\varphi^{(1)}_{1\tau}$$

$$h_2(\bar{X}, \tau) = -\frac{1}{g(\rho_1 - \rho_2)}(\rho_1 \varphi^{(1)}_{1\tau} - \rho_2 \varphi^{(2)}_{1\tau}) \tag{16}$$

4.3. *The third-order approximation*

$$\varphi^{(i)}_{1\bar{X}\bar{X}} + \varphi^{(i)}_{3\bar{Y}\bar{Y}} = 0 \quad (i = 1, 2)$$

$$(\varphi^{(1)}_{3\bar{Y}} - f_{2\tau})_{\bar{Y} = H_1 + H_2} = 0$$

$$(\varphi^{(i)}_{3\bar{Y}} - h_{2\tau})_{\bar{Y} = H_2} = 0 \quad (i = 1, 2)$$

$$(\varphi^{(2)}_{3\bar{Y}})_{\bar{Y} = 0} = 0$$

$$(\varphi^{(i)}_{3\bar{X}})_{\bar{X} = 0} = (\varphi^{(i)}_{3\bar{X}})_{\bar{X} = l} = 0 \quad (i = 1, 2) \tag{17}$$

which finally gives

$$\varphi^{(i)}_3 = -\tfrac{1}{2}B^{(i)}_{\bar{X}\bar{X}}\bar{Y}^2 + C^{(i)}(\bar{X}, \tau)\,\bar{Y} + D^{(i)}(\bar{X}, \tau) \quad (i = 1, 2) \tag{18}$$

where $C^{(i)}$ and $D^{(i)}$ are arbitrary functions which satisfy the following boundary conditions:

$$C^{(2)}(\bar{X}, \tau) \equiv 0; \quad C^{(i)}_{\bar{X}} = 0 \quad \text{for } \bar{X} = 0, l; \quad D^{(i)}_{\bar{X}} = 0 \quad \text{for } \bar{X} = 0, l$$

Introducing eq. (18) in the boundary conditions eq. (17), we get:

$$-(H_1 + H_2)B^{(1)}_{\bar{X}\bar{X}} + C^{(1)} + \frac{1}{g}B^{(1)}_{\tau\tau} = 0$$

$$-H_2 B^{(1)}_{\bar{X}\bar{X}} + C^{(1)} + \frac{1}{g(\rho_1 - \rho_2)}(\rho_1 B^{(1)}_{\tau\tau} - \rho_2 B^{(2)}_{\tau\tau}) = 0$$

$$-H_2 B^{(2)}_{\bar{X}\bar{X}} + \frac{1}{g(\rho_1 - \rho_2)}(\rho_1 B^{(1)}_{\tau\tau} - \rho_2 B^{(2)}_{\tau\tau}) = 0 \tag{19}$$

and by elimination one obtains

$$\Box_1 B^{(1)} = \rho_2 B^{(2)}_{\tau\tau}$$

$$\Box_2 B^{(2)} = \rho_1 B^{(1)}_{\tau\tau} \tag{20}$$

where $\square_1$ and $\square_2$ are the following differential operators:

$$\square_1 \equiv gH_1(\rho_1 - \rho_2)\frac{\partial^2}{\partial \bar{X}^2} + \rho_2 \frac{\partial^2}{\partial \tau^2}$$

$$\square_2 \equiv gH_2(\rho_1 - \rho_2)\frac{\partial^2}{\partial \bar{X}^2} + \rho_2 \frac{\partial^2}{\partial \tau^2}$$

The elimination of $B^{(1)}$ (for example) in (20) gives:

$$\left(\alpha_0 \frac{\partial^2}{\partial \bar{X}^2} + \beta_1 \frac{\partial^2}{\partial \tau^2}\right)\left(\alpha_0 \frac{\partial^2}{\partial \bar{X}^2} + \beta_2 \frac{\partial^2}{\partial \tau^2}\right) B^{(2)} = 0 \tag{21}$$

where

$$\alpha_0 = 2g^2 H_1 H_2(\rho_1 - \rho_2)$$

$$\beta_1 = g\rho_2(H_1 + H_2) + g[\rho_2^2(H_1 + H_2)^2 - 4H_1H_2\rho_2(\rho_2 - \rho_1)]^{1/2}$$

$$\beta_2 = g\rho_2(H_1 + H_2) - g[\rho_2^2(H_1 + H_2)^2 - 4H_1H_2\rho_2(\rho_2 - \rho_1)]^{1/2}$$

Equation (21) has the following general solution:

$$B^{(2)} = T_1(\xi_1) + T_2(\xi_2) + T_3(\xi_3) + T_4(\xi_4) \tag{22}$$

with

$$\xi_1 = \bar{X} - a\tau; \quad \xi_2 = \bar{X} + a\tau; \quad \xi_3 = \bar{X} - b\tau; \quad \xi_4 = \bar{X} + b\tau.$$

and

$$a = -\alpha_0/\beta_1; \quad b = -\alpha_0/\beta_2$$

and T_i ($i = 1, 2, 3, 4$) are arbitrary functions of the variable ξ_i.

4.4. *The fourth-order approximation*

From (7) and (9) we have the following relations:

$$f_4(\bar{X}, \tau) = -\frac{1}{g}\left\{-\frac{(H_1 + H_2)^2}{2} B^{(1)}_{\bar{X}\bar{X}\tau} + (H_1 + H_2)C^{(1)}_\tau + \tfrac{1}{2}(B^{(1)}_{\bar{X}})^2 + D^{(1)}_\tau\right\}$$

$$h_4(X, \tau) = -\frac{1}{g(\rho_1 - \rho_2)}\left\{\begin{aligned}&\rho_1\left[-\frac{H_2^2}{2} B^{(1)}_{\bar{X}\bar{X}\tau} + H_2 C^{(1)}_\tau + \tfrac{1}{2}(B^{(1)}_{\bar{X}})^2 + D^{(1)}_\tau\right]\\ &-\rho_2\left[-\frac{H_2^2}{2} B^{(2)}_{\bar{X}\bar{X}\tau} + \tfrac{1}{2}(B^{(2)}_{\bar{X}})^2 + D^{(2)}_\tau\right]\end{aligned}\right\} \tag{23}$$

4.5. *The fifth-order approximation*

$$\begin{aligned}
&\varphi^{(i)}_{3\bar{X}\bar{X}} + \varphi^{(i)}_{5\bar{Y}\bar{Y}} = 0 \dots (i = 1, 2)\\
&\{\varphi^{(1)}_{5\bar{Y}} - \varphi^{(1)}_{1\bar{X}} f_{2\bar{X}} - f_{4\tau} + f_2 \varphi^{(1)}_{3\bar{Y}\bar{Y}}\}_{\bar{Y} = H_1 + H_2} = 0\\
&\{\varphi^{(i)}_{5\bar{Y}} - \varphi^{(i)}_{1\bar{X}} h_{2\bar{X}} - h_{4\tau} + h_2 \varphi^{(i)}_{3\bar{Y}\bar{Y}}\}_{\bar{Y} = H_2} = 0 \dots (i = 1, 2)\\
&(\varphi^{(2)}_{5\bar{Y}})_{\bar{Y}=0} = 0\\
&(\varphi^{(i)}_{5\bar{X}})_{\bar{X}=0} = (\varphi^{(i)}_{5\bar{X}})_{\bar{X}=l} = 0 \dots (i = 1, 2)
\end{aligned} \tag{24}$$

The above equations lead to

$$\varphi_3^{(i)}(\bar{X},\bar{Y},\tau)=\frac{\bar{Y}^4}{4!}B^{(i)}_{\bar{X}\bar{X}\bar{X}\bar{X}}-\frac{\bar{Y}^3}{3!}C^{(i)}_{\bar{X}\bar{X}}-\frac{\bar{Y}^2}{2}D^{(i)}_{\bar{X}\bar{X}}+\bar{Y}E^{(i)}(\bar{X},\tau)+F^{(i)}(\bar{X},\tau)\ldots(i=1,2) \tag{25}$$

where $E^{(i)}(\bar{X},\tau)$, $F^{(i)}(\bar{X},\tau)$ are arbitrary functions which satisfy the following conditions:

$E^{(2)}(\bar{X},\tau)=0$

$(E^{(1)}_{\bar{X}})_{\bar{X}=0,l}=0$

$(F^{(i)}_{\bar{X}})_{\bar{X}=0,l}=0\ldots(i=1,2)$

Introducing eqs. (16)–(25) in the boundary conditions, we have the following relations:

$$\left\{\begin{aligned}&\frac{(H_1+H_2)^3}{3!}B^{(1)}_{\bar{X}\bar{X}\bar{X}\bar{X}}-\frac{(H_1+H_2)^2}{2!}C^{(1)}_{\bar{X}\bar{X}}-(H_1+H_2)D^{(1)}_{\bar{X}\bar{X}}+E^{(1)}(\bar{X},\tau)+\frac{2}{g}B^{(1)}_{\bar{X}}B^{(1)}_{\bar{X}\tau}\\&+\frac{1}{g}\left\{-\frac{(H_1+H_2)}{2}B^{(1)}_{\bar{X}\bar{X}\tau\tau}+(H_1+H_2)C^{(1)}_{\tau\tau}+D^{(1)}_{\tau\tau}\right\}+\frac{1}{g}B^{(1)}_{\tau}B^{(1)}_{\bar{X}\bar{X}}=0\end{aligned}\right. \tag{26a}$$

$$\left\{\begin{aligned}&\frac{H_2^3}{3!}B^{(1)}_{\bar{X}\bar{X}\bar{X}\bar{X}}-\frac{H_2^2}{2!}C^{(1)}_{\bar{X}\bar{X}}-H_2D^{(1)}_{\bar{X}\bar{X}}+E^{(1)}+\frac{1}{g(\rho_2-\rho_1)}B^{(1)}_{\bar{X}}[\rho_2B^{(2)}_{\bar{X}\tau}-\rho_1B^{(1)}_{\bar{X}\tau}]\\&+\frac{1}{g(\rho_2-\rho_1)}\left\{\rho_2\left[-\frac{H_2^2}{2}B^{(2)}_{\bar{X}\bar{X}\tau\tau}+D^{(2)}_{\tau\tau}\right]-\rho_1\left[-\frac{H_2^2}{2}B^{(1)}_{\bar{X}\bar{X}\tau\tau}+H_2C^{(1)}_{\tau\tau}+D^{(1)}_{\tau\tau}\right]\right.\\&\left.+\rho_2B^{(2)}_{\bar{X}}B^{(2)}_{\bar{X}\tau}-\rho_1B^{(1)}_{\bar{X}}B^{(1)}_{\bar{X}\tau}\right\}+\frac{1}{g(\rho_2-\rho_1)}B^{(1)}_{\bar{X}\bar{X}}(\rho_2B^{(2)}_{\tau}-\rho_1B^{(1)}_{\tau})=0\end{aligned}\right. \tag{26b}$$

$$\left\{\begin{aligned}&\frac{H_2^3}{3!}B^{(2)}_{\bar{X}\bar{X}\bar{X}\bar{X}}-H_2D^{(2)}_{\bar{X}\bar{X}}+\frac{1}{g(\rho_2-\rho_1)}B^{(2)}_{\bar{X}}[\rho_2B^{(2)}_{\bar{X}\tau}-\rho_1B^{(1)}_{\bar{X}\tau}]\\&+\frac{1}{g(\rho_2-\rho_1)}\left\{\rho_2\left[-\frac{H_2^2}{2}B^{(2)}_{\bar{X}\bar{X}\tau\tau}+D^{(2)}_{\tau\tau}\right]-\rho_1\left[-\frac{H_2^2}{2}B^{(1)}_{\bar{X}\bar{X}\tau\tau}+H_2C^{(1)}_{\tau\tau}+D^{(1)}_{\tau\tau}\right]+\rho_2B^{(2)}_{\bar{X}}B^{(2)}_{\bar{X}\tau}\right.\\&\left.-\rho_1B^{(1)}_{\bar{X}}B^{(1)}_{\bar{X}\tau}\right\}+\frac{1}{g(\rho_2-\rho_1)}B^{(2)}_{\bar{X}\bar{X}}(\rho_2B^{(2)}_{\tau}-\rho_1B^{(1)}_{\tau})=0\end{aligned}\right. \tag{26c}$$

We have six unknown functions and a system of six partial differential equations (19) and (26). We now focus attention on progressive waves and standing waves.

5. The progressive wave

We have seen in (22) that $B^{(i)}=\sum_{k=1}^{4}T_k^{(i)}(\xi_k)$. We choose a pure progressive wave, i.e. $B^{(i)}=B^{(i)}(\xi_1)$, for example, with $\xi_1=\xi=\bar{X}-c\tau$, where c can take the two possible values a or b as defined in (22). Let $a<b$ so that a will describe the baroclinic mode and b the barotropic. We let

$$B^{(i)}(\bar{X},\tau)=B^{(i)}(\bar{X}-c\tau)=B^{(i)}(\xi) \tag{27}$$

and substituting this in eq. (19) leads to

$$B^{(1)}(\xi) = \frac{1}{\lambda} B^{(2)}(\xi)$$

$$C^{(1)} = \gamma B^{(1)}_{\xi\xi} \tag{28}$$

with

$$\lambda = \frac{c^2 - gH_1}{gH_2} \quad \text{and} \quad \gamma = H_1 + H_2 - \frac{c^2}{g}$$

The elimination of $E^{(1)}$ in eqs. (26) gives the following system of differential equations:

$$\left(H_1 - \frac{c^2 \rho_2}{g(\rho_2 - \rho_1)}\right) D^{(1)}_{\xi\xi} + \frac{c^2 \rho_2}{g(\rho_2 - \rho_1)} D^{(2)}_{\xi\xi} = P_1 B^{(1)}_{\xi\xi\xi\xi} + Q_1 B^{(1)}_{\xi} B^{(1)}_{\xi\xi}$$

$$\frac{c^2 \rho_1}{g(\rho_2 - \rho_1)} D^{(1)}_{\xi\xi} + \left(H_2 - \frac{c^2 \rho_2}{g(\rho_2 - \rho_1)}\right) D^{(2)}_{\xi\xi} = P_2 B^{(1)}_{\xi\xi\xi\xi} + Q_2 B^{(1)}_{\xi} B^{(1)}_{\xi\xi} \tag{29}$$

Coefficients P_1, P_2, Q_1 and Q_2 are given in Appendix A_1. This system is a linear system for the functions $D^{(i)}$ and the homogeneous part of eq. (29) is similar to (20). In (20), since we choose the correct value of c (a or b), the principal determinant is zero as is the principal determinant of (29). Since we require a non-trivial solution for (29), the secondary determinant must be zero, which leads to the following differential equation for $B^{(1)}$:

$$\left[\left(H_2 - \frac{c^2 \rho_2}{g(\rho_2 - \rho_1)}\right) P_1 - \frac{\rho_2 c^2}{g(\rho_2 - \rho_1)} P_2\right] B^{(1)}_{\xi\xi\xi\xi} + \left[\left(H_2 - \frac{c^2 \rho_2}{g(\rho_2 - \rho_1)}\right) Q_1 - \frac{c^2 \rho_2}{g(\rho_2 - \rho_1)} Q_2\right] B^{(1)}_{\xi} B^{(1)}_{\xi\xi} = 0$$

By changing the variables $Y = B^{(1)}_{\xi}$ eq. (30) becomes the following Boussinesq equation:

$$\mathscr{M}_1 Y''' + \mathscr{M}_2 YY' = 0 \quad \text{where} \quad Y' = Y_{\xi}, \quad Y'' = Y_{\xi\xi}, \cdots \tag{31}$$

Coefficients $\mathscr{M}_1$ and $\mathscr{M}_2$ are given in Appendix A_1. After two integrations eq. (31) becomes

$$(Y')^2 = AY^3 + pY + q = P_3(Y) \tag{32}$$

where $A = -\mathscr{M}_1/3\mathscr{M}_2$ and p, q are arbitrary constants. As A is always different from zero, $P_3(Y)$ is a polynomial function of the third order. In our physical problem, Y must be a bounded function for $-\infty < \xi < +\infty$. This imposes that the poles of P_3 must be real. Therefore

$$P_3(Y) = A[(Y - Y_1)(Y - Y_2)(Y - Y_3)]$$

and Y_1, Y_2, Y_3 are chosen such as $Y_1 > Y_2 > Y_3$. The general solution of eq. (32) can be found in Byrd and Friedmann (1954) in terms of Jacobi elliptic function $\mathrm{sn}(u, k^2)$.

$$Y = Y_1\left[1 - \frac{3k^2}{1 + k^2} \mathrm{sn}^2\left(2K\frac{\xi}{\Lambda}, k^2\right)\right] \tag{33}$$

with the wavelength Λ defined by:

$$\Lambda = 4K(k^2)\sqrt{\frac{(1 + k^2)}{-3AY_1}} \tag{34}$$

where $K(k^2)$ is the complete elliptic integral of the first kind, and $B^{(1)}$ can be found by integrating eq. (33):

$$B^{(1)}(\xi) = \left[Y_1 - \frac{6(K - E)}{2K(1 + k^2)}\right]\xi + \frac{6}{\sqrt{-3AY_1(1 + k^2)}} Z\left(\frac{2K\xi}{\Lambda}, k^2\right) \tag{35}$$

where $Z(u, k^2)$ is the Zeta Jacobi elliptic function and $E(k)$ is the complete elliptic integral of the second kind, but is of less interest than $Y = B_\xi^{(1)}$ because from (16)

$$f_2(\bar{X}, \tau) = \frac{c}{g} B_\xi^{(1)}(\xi)$$

$$h_2(\bar{X}, \tau) = \left(\frac{\rho_1 - \lambda\rho_2}{\rho_1 - \rho_2}\right) \frac{c}{g} B_\xi^{(1)}(\xi) \tag{36}$$

and from (11), h_2 and f_2 are the first terms in the expansion of h and f.

6. The standing wave

We return to the initial problem, an internal wave in a rectangular tank.

6.1. *Introduction of the boundary conditions at the end of the tank*

For a standing wave we impose the boundary conditions

$$(\varphi_{1X}^{(i)})_{\bar{X}=0,l} = 0 \cdots (i = 1, 2) \tag{37}$$

Using (37) and the principle of symmetry, we can extend the solution to the domain $-\infty < \bar{X} < +\infty$ and obtain the new relations:

$$\varphi_{1X}^{(i)}(\bar{X}, \tau) = \varphi_{1X}^{(i)}(\bar{X} + 2l, \tau) \cdots -\infty < \bar{X} < \infty \tag{38}$$

Equation (38) implies that $\varphi_{1X}^{(i)}$ is a spatial periodic function of period $2l$. As we have seen in (22), the general solution is of the form

$$\varphi_1^{(i)}(\bar{X}, \tau) = B^{(i)}(\bar{X}, \tau) = \sum_{k=1}^{4} T_k^{(i)}(\xi_k)$$

We now focus our attention on the case where the baroclinic and barotropic mode do not interact, i.e. $2l/a \neq n(2l/b)$ (this condition raises some mathematical difficulties and will not be pursued further). In this case the standing wave will be described by:

$$B^{(i)}(\bar{X}, \tau) = T_1^{(i)}(\bar{X} - c\tau) + T_2^{(i)}(\bar{X} + c\tau) \cdots (i = 1, 2) \tag{39}$$

where c can take the values a or b. Here,

$$B_X^{(i)} = T_{1X}^{(i)}(\xi_1) + T_{2X}^{(i)}(\xi_2) \cdots (i = 1, 2) \quad \begin{cases} \xi_1 = \bar{X} - c\tau \\ \xi_2 = \bar{X} + c\tau \end{cases} \tag{40}$$

From (37)

$$T_{1X}^{(i)}(u) = -T_{2X}^{(i)}(-u) \cdots (i = 1, 2)$$

so (40) leads to

$$B_X^{(i)} = T_{1X}^{(i)}(\xi_1) - T_{1X}^{(i)}(-\xi_2) \ldots (i = 1, 2) \tag{41}$$

Integrating (41) we obtain:

$$B^{(i)}(\bar{X}, \tau) = T_1^{(i)}(\xi_1) + T_1^{(i)}(-\xi_2) \ldots (i = 1, 2) \tag{42}$$

Considering that in this case we also have $B_{XX}^{(i)} = (1/c^2)B_{\tau\tau}^{(i)}$, we arrive at the same relations as (28), i.e.

$$B^{(2)} = \lambda B^{(1)}$$

$$C^{(1)} = \gamma[T_{1\xi\xi}^{(1)}(\xi_1) + T_{1\xi\xi}^{(1)}(-\xi_2)] = \gamma B_{\xi\xi}^{(1)} \tag{43}$$

Introducing these new relations in (26), we arrive at

$$\square_2\square_1 D^{(1)} - \rho_1\rho_2 D^{(1)}_{\tau\tau\tau\tau} = \square_2(F_1 - F_2) + \rho_2 F_{3\tau\tau} \tag{44}$$

where $\square_1$, $\square_2$ are the differential operators defined in (20), and F_1, F_2, F_3 are defined in Appendix A_1. Integration of eq. (44) leads to the following relation:

$$\begin{aligned}\psi(\xi_1,\xi_2) = {} & \xi_2\{\mathcal{M}_1 T_1^{V}(\xi_1) + \mathcal{M}_2[T_1'''(\xi_1)T_1'(\xi_1) + (T_1''(\xi_1))^2]\} \\ & + \xi_1\{-\mathcal{M}_1 T_1^{V}(-\xi_2) - \mathcal{M}_2[T_1'''(-\xi_2)T_1'(-\xi_2) + (T_1''(-\xi_2))^2]\} + G_1(\xi_1) + G_2(\xi_2) \\ & + \mathcal{M}_3[-T_1(\xi_1)T_1'''(-\xi_2) - T_1(-\xi_2)T_1'''(\xi_1)] + \mathcal{M}_4[-T_1''(\xi_1)T_1'(-\xi_2) - T_1'(\xi_1)T_1''(-\xi_2)]\end{aligned} \tag{45}$$

where

$$\psi = \left(b^2\frac{\partial^2}{\partial \bar{X}^2} - \frac{\partial^2}{\partial Z^2}\right)D,$$

$\mathcal{M}_1$ and $\mathcal{M}_2$ are defined in Appendix A_1 (they are the same as for progressive waves). $\mathcal{M}_3$ and $\mathcal{M}_4$ are constants and $G_1(\xi_1)$ $G_2(\xi_2)$ are arbitrary functions. The transition from eq. (44) to eq. (45) involves tedious calculus which has not been reproduced in this paper. It can be found in Helal (1979).

Since were required ψ to be a bound function, we may assume that the secular terms are null. This leads to the following equations:

$$\begin{cases}\mathcal{M}_1 T_1^{V}(\xi_1) + \mathcal{M}_2(T_1''(\xi_1)T_1'(\xi_1))' = 0 \\ \mathcal{M}_1 T_1^{V}(-\xi_2) + \mathcal{M}_2[T_1''(-\xi_2)T_1'(-\xi_2)]' = 0\end{cases} \tag{46}$$

By successive integrations eq. (46) leads to

$$\begin{aligned}&\mathcal{M}_1 Y_1''' + \mathcal{M}_2 Y_1' Y_1 = 0 \\ &\mathcal{M}_1 Y_2''' + \mathcal{M}_2 Y_2' Y_2 = 0\end{aligned} \tag{47}$$

where $Y_1 = T_1'(\xi_1)$ and $Y_2 = T_1'(-\xi_2)$. This is the Boussinesq equation found in (31). We have already found the general solution of this equation, and from (4), using (41), we arrive at the final form

$$f_2(\bar{X},\tau) = -\frac{1}{g}B^{(1)}_{\tau}$$

$$h_2(\bar{X},\tau) = -\frac{1}{g}\left(\frac{\rho_1 - \lambda\rho_2}{\rho_1 - \rho_2}\right)B^{(1)}_{\tau}$$

and

$$B^{(1)} = T_1(\xi_1) + T_1(-\xi_2) \tag{48}$$

which describe the system of standing waves.

Some details on the computation, for the physical problem, of the different parameters which appear in the Jacobi elliptic function are given in Appendix A_2.

Fig. 2 gives the general features of the solutions described by (48). Also of note is the fact that in the baroclinic mode the ratio between the surface wave amplitude and internal wave amplitude is of the order of

$$\frac{H_2}{H_1 + H_2}\frac{\Delta\rho}{\rho_2} = \frac{A_s}{A_i}$$

which is always less than $\Delta\rho/\rho_2$ (in our experiments $\Delta\rho/\rho_2$ never exceeds 1.5%). In Fig. 2a, the vertical scale is exaggerated by about 100-fold for the surface wave. For the barotropic mode, A_s/A_i is of the order of 1.

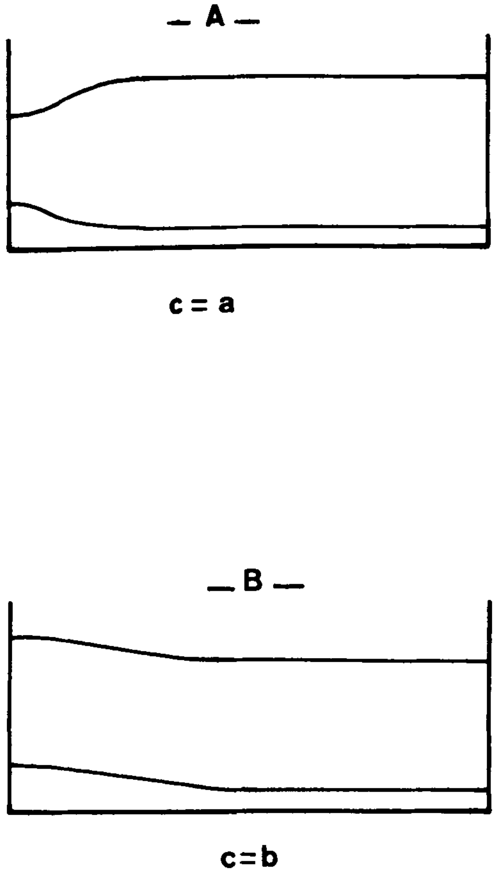

Fig. 2. Theoretical solution calculated for $H_1 = 25$ cm, $H_2 = 5$ cm, $\Delta\rho/\rho_2 = 1.3\%$. Internal wave amplitude $A_i = 3$ cm. (A) Baroclinic mode. Note that the surface wave amplitude had been emphasized to about 100, compare with the internal wave amplitude. (B) Barotropic mode. Same scale for internal and surface wave.

7. Experimental apparatus

We have performed laboratory experiments to test the theoretical results on the wave shape with respect to t. Figs. 3, 4 and 5 describe the different apparatus involved in the experiment.

The apparatus (Fig. 3) consists of a 2.03 m long, glass-walled rectangular tank (C), 0.40 m high and 0.50 m wide. The tank can be rotated around an horizontal axis (D) at any period between 10 s and 150 s. This period will be called T_{ex}. The oscillations of the tank are generated by an eccentric drive system (E) consisting of an electric motor, a group of reduction gears and a magnetic clutch. The precision of the period is better than 1‰. It is the oscillation of the tank at the eigen period of the internal wave which generates the internal wave. The maximum angle of tilt of the tank can be adjusted from 0 to 0.5 rd but generally we use angles of less than 0.002 rd in order to avoid the effect of a bottom slope which has not been taken into consideration in the theory. The tank is filled with two layers of fluids which are: (A) fresh water, (B) brine which is dyed for good visualization of the wave.

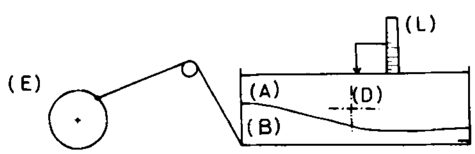

Fig. 3. General scheme of the experimental device.

The tank is first filled with fresh water of depth H_1, controlled by a point gauge (L) (precision 0.1 mm) and is then immobilized with the brine inlet at the low point (Fig. 4).

The brine is introduced through a perforated pipe (P), below a plastic-made rule (R) which is placed 1 mm from the bottom of the tank. This rule allows laminar brine flow. Filling is completed when a height of $H_1 + H_2$ is measured by the point gauge (L). The smallest relative density difference can be about 0.5% but for all experiments presented here $\Delta\rho/\rho_2 = 1.38\% \pm 0.05\%$. With such a difference the interface thickness is 0.60 cm $\pm$ 0.1 cm at the end of the filling operation.

The internal waves are measured with an interface follower. This apparatus is able to follow the movement of a layer of given conductivity with great accuracy. A more precise description of this apparatus can be found in Suberville (1974). Basically, the principle of this apparatus is to measure the conductivity and to compare it with a given reference (chosen by the experimenter) (Fig. 5a).

A small electric motor is slaved to move the conductivity probe in order to make the difference between the measured and reference conductivity as small as possible. With this system we are able to follow the interface with a precision of 0.1 mm in height, and response time of about 0.5 s. The conductivity probe is a small tube (Fig. 5b) through which the fluid is drawn. Three electrodes allow the measurement of the resistance and the capacity of the column of the fluid which has been drawn off (the fluid discharge is very small, about 0.05 $cm^3\ s^{-1}$). With this kind of probe we avoid the adverse effects introduced by the inner sides of the tank and by other conductivity probes in the same fluid.

The recording can be made in two ways.

(i) Analogue recording from a rotary potentiometer, fitted on the same axis as the motor.
(ii) A digital optical coder (10,000 points per revolution), fitted on the same axis as the motor, allows direct data acquisition on a micro-computer HP 9845B with a sample of 152 points per period of the wave.

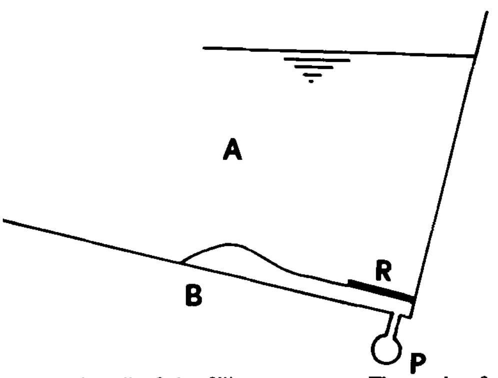

Fig. 4. Detail of the filling apparatus. The angle of tilt has been exaggerated.

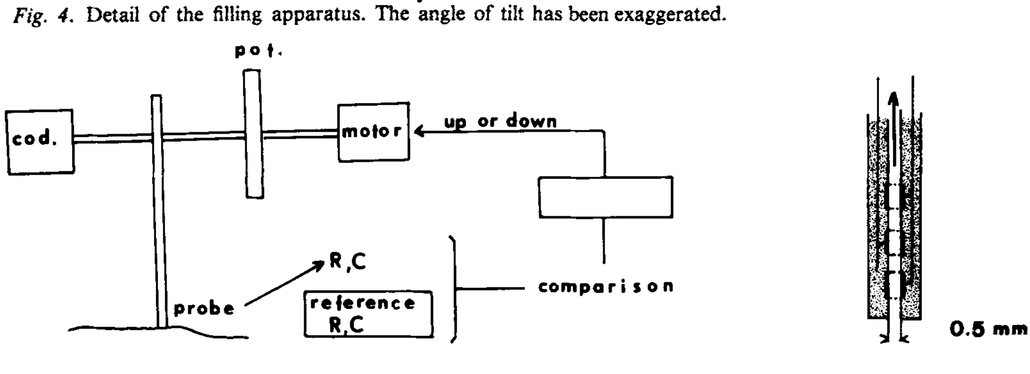

Fig. 5. (a) Synoptic scheme of the interface follower. (b) Detail of the probe.

Data acquisition is synchronized with tank movement and this allows good spatial coverage of the experiments and enables experiments to be repeated and probes to be moved. Each experiment is performed with $H_1 + H_2 = 30$ cm; only the ratio H_1/H_2 changes. As previously mentioned, the density difference is made constant with $\Delta\rho/\rho_2 = 1.38\% \pm 0.05\%$. Consequently, we can make a good comparison between different experiments.

8. Experimental results

8.1. *Periods*

The period of the internal waves depends on several parameters, some of which have not been taken into consideration in the theory:

(i) interface thickness,
(ii) viscosity (dissipation),
(iii) wave reflection at the end of the tank,
(iv) wave amplitude.

Let us see what are the effects of these parameters on the period of the internal standing wave. Suberville (1974) showed that when the interface thickness increases, the period also increases. Physically, the dissipation (which comes from friction) decreases the celerity of the waves and thus increases the wave period in our case. The effect of wave reflection has been studied both theoretically and experimentally for free surface waves by Temperville (1975) and Maxworthy (1976). They found that, for non-linear waves, the wave reflection introduces a phase-shift, so that the period must increase. For non-linear internal waves, although no calculations are available, the phenomenon should have the same tendency. Lastly, several authors have shown numerically (e.g. Meiss and Pereira, 1978) and theoretically (Lee and Beardsley, 1974) that the celerity of non-linear internal waves increases as its amplitude increases. It has also been observed in the ocean (e.g. Apel et al., 1980).

It is therefore difficult to make any comparison between the theoretical period and the physical period. It is also difficult to measure the eigen period (T_0) of the wave in highly non-linear cases (H_1 very different from H_2) because of the dissipation, as the period increases when the wave amplitude decreases. We have thus chosen a very sensitive parameter, the phase-shift between the wave and the oscillation of the tank, to describe whether or not the excitation period corresponds to the eigen period of the wave. Since we have seen in previous experiments that in the case of a linear sine shape wave ($H_1 = H_2 = 15$ cm) the excitation period and the eigen period correspond when the phase-shift is equal to 90°, then we have assumed that this phase-shift (90°) gives the condition of equality between the two periods even for highly non-linear internal waves.

We have made some experiments in which the excitation period is slightly varied around the period T_0 for which the phase-shift was 90°. The following features are brought to attention (Fig. 6):

For $T_{ex} > T_0$ we obtain a stable phenomenon with a constant phase-shift greater than 90°, and the wave shape is considerably altered in comparison with the case where $T_0 = T_{ex}$. In highly non-linear cases, one or more (up to four) secondary crests appear and the wave takes the shape of a multi-soliton wave. In our case this type of wave must be taken up using the periodic solutions of the Korteweg–de Vries equation.

8.2. *The wave shape $h(t, x_0)$ where x_0 is a constant abscissa*

The observed wave takes the shape as shown in Fig. 7a.

We have shown experimentally that the wave (Fig. 7a) is a linear superposition of a cnoidal shape wave (Fig. 7c) (90° phase-shift), and a sine shape wave (Fig. 7b) (0° phase-shift). The fact that the sine shape wave has a 0° phase-shift clearly indicates that this sine shape wave is linked with the oscillation of the tank (some calculations must be made to prove this assumption). As we have seen in Fig. 6, if we decrease the period of excitation the wave tends to become a 0° phase-shift sine shape

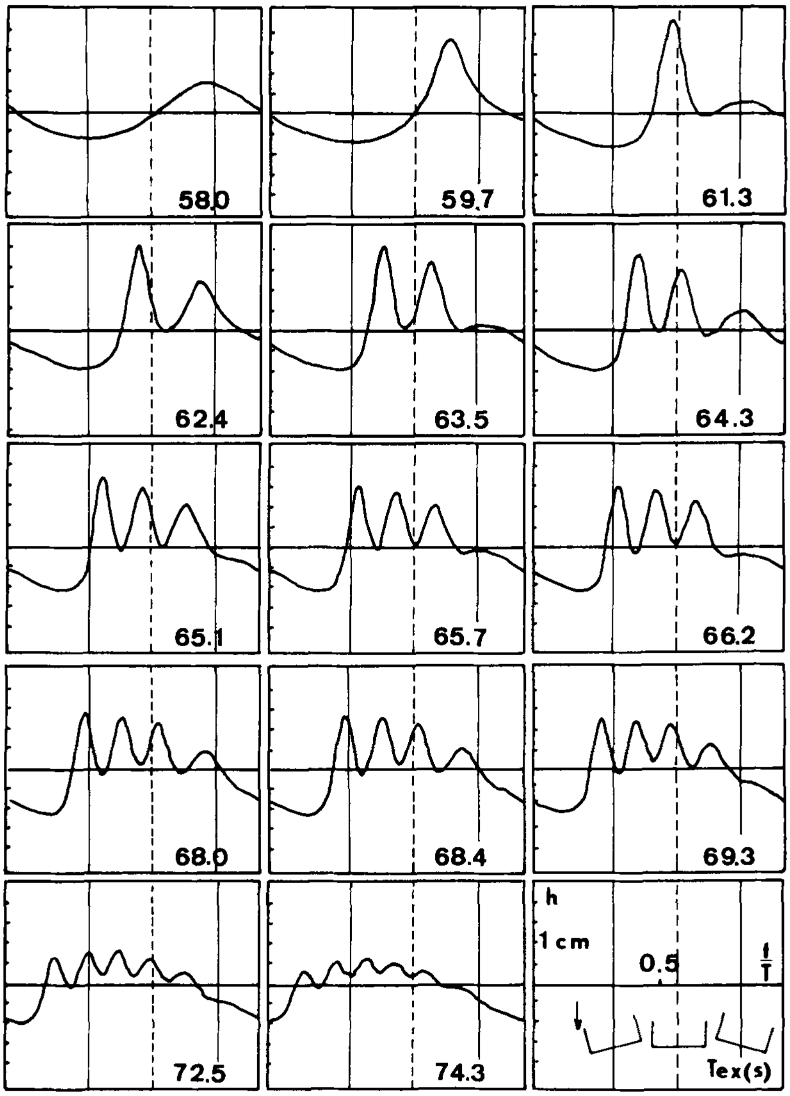

Fig. 6. Evolution of the wave shape according to the excitation period. Experiments have been conducted with $H_1 = 26$ cm, $H_2 = 4$ cm, $\Delta\rho/\rho_2 = 1.34\%$. The eigen period of the wave is 60.9 s. For all figures the amplitude of the excitation is the same and equal to 0.004 rd. The scales and legend of the figures are indicated in the lower right corner.

wave, i.e. the cnoidal shape wave (7b) vanishes because it was not excited at its eigen period. We have shown that if $(T_0 - T_{ex})/T_0 > 7\%$ the cnoidal shape wave is less than 1% of the sine shape wave. So we suppose that the recording done with $(T_0 - T_{ex})/T_0 \simeq 7\%$ gives us a good enough approximation of the sine shape wave (7b). Consequently we have made the comparison between the cnoidal shape wave (obtained by making the difference between (7a) and (7b)) and the theory. As the difference is made point by point, with 152 points per period, the problem of the difference between the experimental period and theoretical period has been bypassed. A sample of the most significant results is shown below (Fig. 8).

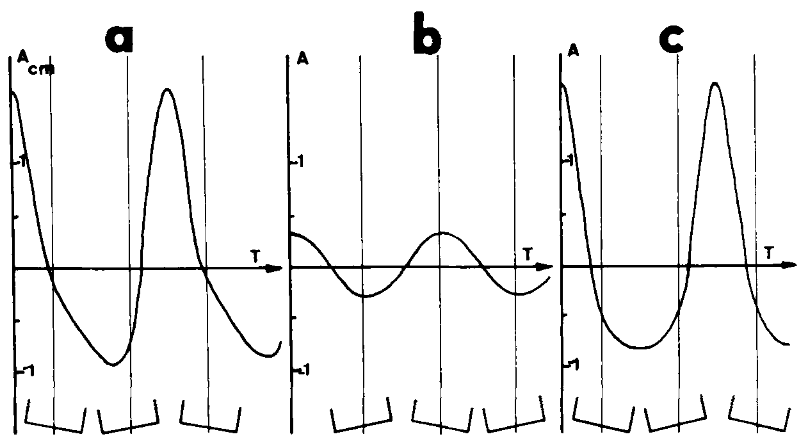

Fig. 7. (a) Observed wave, phase-shift $\simeq 90°$. (b) Sine shape wave, phase-shift $= 0°$. (c) Difference between (a) and (b). Note that the position of the tank in function of time has been drawn schematically. The probe location is on the left side of the tank.

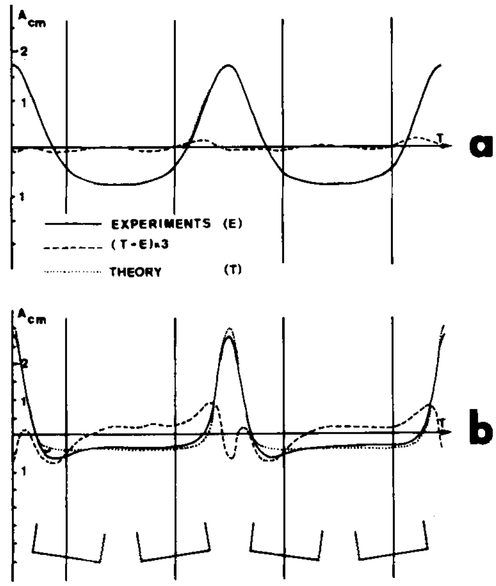

Fig. 8. Comparison between theory and experiments.
(a) $H_1 = 20$ cm, $H_2 = 10$ cm $\Delta\rho/\rho_2 = 1.34\%$, $A_I = 2.5$ cm. $k^2 = 0.971928$; the two graphs are quite similar.
(b) $H_1 = 25$ cm, $H_2 = 5$ cm $\Delta\rho/\rho_2 = 1.34\%$, $A_I = 3.5$ cm. $k^2 = 0.999999$.

9. Conclusion

In order to have a general viewpoint of the different experiments we have calculated the average standard deviation σ for the amplitudes between theory and experiment, for each experiment. In addition, the non-linear effects have been estimated with the parameter $\alpha = A_I|H_1 - H_2|/(H_1 + H_2)^2$ (Miles, 1979) (A_I is the internal wave amplitude). Fig. 9 shows the graph of σ/A_I as a function of α. The graph of σ/A_I as a function of H_r/H_I where $H_r = H_1 H_2/H_1 + H_2$ has also been plotted (Fig. 10).

These latter graphs show some dispersion of the results. This dispersion is certainly introduced by experimental difficulties such as interface thickness, but it can be seen that all the experiments give a ratio σ/A_I within 5%. From these results and especially from figures such as Fig. 8, we can say that our solution in eq. (48) represents the main features of a non-linear internal standing wave.

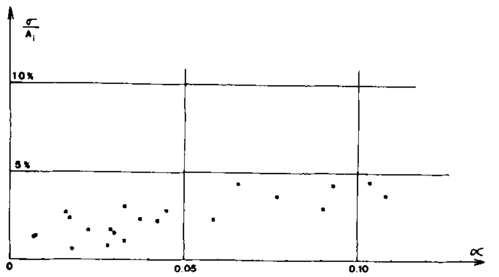

Fig. 9. Graph of σ/A_i as a function of $\alpha = A_i \dfrac{|H_1 - H_2|}{(H_1 + H_2)^2}$.

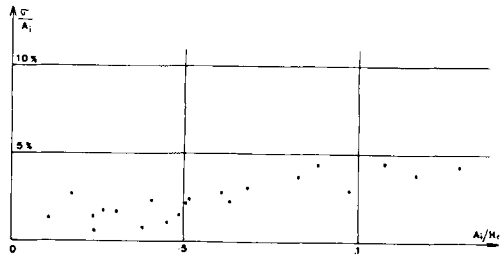

Fig. 10. Graph of σ/A_i as a function of H_r/A_i where $H_r = \dfrac{H_1 H_2}{H_1 + H_2}$.

10. Acknowledgements

We are grateful to Pr. J. P. Germain, A. Temperville, G. Chabert d'Hières and D. Renouard who brought helpful advice to this work. We wish to thank the Egyptian Government and the C.N.R.S. which gave us financial support for this work. The authors also express their gratitude to the referees for the careful and helpful review.

11. Appendix A_1

Equations (30) and (45) introduce the following coefficients:

$$\mathcal{M}_1 = \left(H_2 - \frac{c^2 \rho_2}{g(\rho_2 - \rho_1)} \right) P_1 - \frac{c^2 \rho_2}{g(\rho_2 - \rho_1)} P_2$$

$$\mathcal{M}_2 = \left(H_2 - \frac{c^2 \rho_2}{g(\rho_2 - \rho_1)} \right) Q_1 - \frac{c^2 \rho_2}{g(\rho_2 - \rho_1)} Q_2$$

with

$$P_1 = \frac{[(H_1 + H_2)^3 - H_2^3]}{3!} - \frac{\gamma}{2}[(H_1 + H_2)^2 - H_2^2] - \frac{(H_1 + H_2)^2 c^2}{2g} + \frac{(H_1 + H_2)}{g} \gamma c^2$$

$$+ \frac{c^2}{2g(\rho_2 - \rho_1)} (H_2^2 \rho_2 \lambda - \rho_2 H_2^2 + 2H_2 \rho_1 \gamma)$$

$$P_2 = \frac{\lambda H_2^3}{3!} - \frac{c^2}{2g(\rho_2 - \rho_1)} (H_2^2 \rho_2 \gamma - \rho_1 H_2^2 + 2H_2 \rho_1 \gamma)$$

$$Q_1 = \frac{c}{g(\rho_2 - \rho_1)} ((\lambda + 2)\lambda \rho_2 - 3\rho_1) - \frac{3c}{g}$$

and

$$Q_2 = \frac{c}{g(\rho_2 - \rho_1)} (-3\lambda^2 \rho_2 + (2\lambda + 1)\rho_1)$$

Equation (44) introduces the following functions:

$$F_1 = -\frac{(H_1+H_2)^3}{3!} B^{(1)}_{XXXX} + \frac{(H_1+H_2)^2}{2!} C^{(1)}_{XX} - \frac{2}{g} B^{(1)}_{X} B^{(1)}_{X\tau} + \frac{(H_1+H_2)^2}{2g} B^{(1)}_{XX\tau\tau}$$

$$-\frac{(H_1+H_2)}{g} C^{(1)}_{\tau\tau} - \frac{1}{g} B^{(1)}_{XX} B^{(1)}_{\tau};$$

$$F_2 = -\frac{H_2^3}{3!} B^{(1)}_{XXXX} + \frac{H_2^2}{2!} C^{(1)}_{XX} + \frac{B^{(1)}_X}{g(\rho_1-\rho_2)} (\rho_2 B^{(2)}_{X\tau} - \rho_1 B^{(1)}_{X\tau})$$

$$+\frac{1}{g(\rho_1-\rho_2)} \left[-\rho_2 \frac{H_2^2}{2} B^{(2)}_{XX\tau\tau} - \rho_1 \left(-\frac{H_2^2}{2} B^{(1)}_{XX\tau\tau} + H_2 C^{(1)}_{\tau\tau} \right) + \rho_2 B^{(2)}_{X\tau} B^{(2)}_{X} - \rho_1 B^{(1)}_{X} B^{(1)}_{X\tau} \right]$$

$$+\frac{B^{(1)}_{XX}}{g(\rho_1-\rho_2)} (\rho_2 B^{(2)}_{\tau} - \rho_1 B^{(1)}_{\tau})$$

and

$$F_3 = -\frac{H_2^3}{3!} B^{(2)}_{XXXX} + \frac{B^{(2)}_X}{g(\rho_1-\rho_2)} (\rho_2 B^{(2)}_{X\tau} - \rho_1 B^{(1)}_{X\tau}) + \frac{1}{g(\rho_1-\rho_2)}$$

$$\left[-\rho_2 \frac{H_2^2}{2} B^{(2)}_{XX\tau\tau} - \rho_1 \left(-\frac{H_2^2}{2} B^{(1)}_{XX\tau\tau} + H_2 C^{(1)}_{\tau\tau} \right) + \rho_2 B^{(2)}_{X\tau} B^{(2)}_{X} - \rho_1 B^{(1)}_{X} B^{(1)}_{X\tau} \right]$$

$$+\frac{B^{(2)}_{XX}}{g(\rho_1-\rho_2)} (\rho_2 B^{(2)}_{\tau} - \rho_1 B^{(1)}_{\tau})$$

12. Appendix A_2

In order to calculate numerical values to make the comparison between the theory and experiments, we must return to the initial variables x, y, t. To the second order we have the relation:

$$h(\bar{X}, \tau) = H_2 + \varepsilon^2 h_2(\xi) + O(\varepsilon^4) = H(x, t) + O(\varepsilon^4) \tag{A.1}$$

so

$$H(x, t) = H_2 + \varepsilon^2 h_2[\varepsilon(x - ct)]$$

From (48) and (A.1), the wave amplitude is A_l:

$$A_l = \mu \left(\frac{\rho_1 - \lambda\rho_2}{\rho_1 - \rho_2} \right) \frac{c}{g} Y_1 \varepsilon^2 \left(\frac{3k^2}{1+k^2} \right) \tag{A.2}$$

with $\mu = 1$ for progressive wave, and $\mu = 2$ for standing wave. The wavelength is Λ_0:

$$\Lambda_0 = \frac{\Lambda}{\varepsilon} = 4K(k^2) \sqrt{\frac{(1+k^2)}{-3AY_1\varepsilon^2}} \tag{A.3}$$

By elimination of the product $Y_1 \varepsilon^2$ in (A.2) and (A.3), we arrive at the following relation:

$$k^2 K^2(k^2) = A_l \frac{\Lambda_0^2 A g(\rho_2 - \rho_1)}{16\mu c(\lambda\rho_2 - \rho_1)}$$

All the parameters in this relation are known as soon as the four basic parameters H_1, H_2, ρ_1 and ρ_2 are known. In the case of a standing wave, and for our experiments, the wavelength Λ_0 is twice the length of the tank. The function $K^2 k^2$ is monotonic crescent of the variable k^2 so that the product $K^2 k^2$ gives the corresponding value of k^2 and from eq. (A.2) we can determine the product $Y_1 \varepsilon^2$. For the first-order approximation we have not used the value of ε, but for higher approximation it must be arbitrarily chosen (e.g. $\varepsilon = H/L$).

REFERENCES

Apel, J. R., Byrne, H. M., Proni, J. R. and Charnell, R. L. 1975. Observation of oceanic internal wave and surface wave from the earth resources technology satellite. *J. Geophys. Res. 80*, 865–881.

Benjamin, T. B. 1967. Internal waves of permanent form in fluids of great depth. *J. Fluid Mech. 29*, 559–592.

Benney, D. J. and Ko, D. R. S. 1978. The propagation of long, large amplitude internal waves. *Studies in Appl. Math. 59*, 187–199.

Boussinesq, M. J. 1871. Théorie de l'intumescence liquide appelée onde solitaire ou de translation, se propageant dans un canal rectangulaire. *Acad. Sci. Paris Comptes Rendus 72*, 755–759.

Byrd, P. F. and Friedmann, H. D. 1954. *Handbook of elliptic integral for engineering and physicists.* Berlin: Springer-Verlag, 355 pp.

Chabert d'Hières, G. and Suberville, J. L. 1974. Ondes internes à l'interface de deux fluides de densités voisines contenus dans un bassin rectangulaire tournant. *La Houille Blanche 7/8*, 623–629.

Davis, R. E. and Acrivos, A. 1967. Solitary internal waves in deep water. *J. Fluid Mech. 29*, 593–607.

Djordjevic, V. D. and Redekopp, L. G. 1978. The fission and disintegration of internal solitary waves moving over two-dimensional topography. *J. Phys. Oceanogr. 8*, 415–431.

Farmer, D. M. 1978. Observations of long non-linear internal waves in a lake. *J. Phys. Oceanogr. 8*, 63–73.

Grimshaw, R. 1972. Non-linear internal gravity waves in a slowly varying medium. *J. Fluid Mech. 54*, 193–207.

Grimshaw, R. 1978. Long non-linear internal waves in channel of arbitrary cross section. *J. Fluid Mech. 86*, 415–431.

Helal, M. 1979. Application de la théorie de l'eau peu profonde au cas des fluides en bicouches et des fluides en milieu tournant. Doctoral Thesis. Université de Grenoble I.

Hunkins, K. and Fliegel, M. 1973. Internal undular surges in Seneca lake: A natural occurrence of solitons. *J. Geophys. Res. 78*, 539–548.

Kakutani, T. and Yamasaki, N. 1978. Solitary waves on a two-layer fluid. *J. Phys. Soc. Japan 45*, 674–679.

Keulegan, M. J. 1953. Characteristics of internal solitary waves. *J. Res. Natl. Bur. Stand. 51*, 133–140.

Korteweg, D. J. and de Vries, G. 1895. On the change of form of long waves advancing in a rectangular canal and on a new type of long stationary waves. *Phil. Mag. 39*, 422–443.

Lee, C. Y. and Beardsley, R. C. 1974. The generation of long, non-linear internal waves in a weakly stratified shear flow. *J. Geophys. Res. 79*, 453–462.

Long, R. R. 1956. Solitary waves in one- and two-fluid systems. *Tellus 8*, 460–471.

Maxworthy, T. 1976. Experiments on collision between solitary waves. *J. Fluid Mech. 76*, 177–185.

Maxworthy, T. 1979. A note on the internal solitary wave produced by tidal flow over a three-dimensional ridge. *J. Geophys. Res. 84*, 338–346.

Meiss, J. D. and Pereira, N. R. 1978. Internal waves solitons. *Phys. Fluids 21*, 700–702.

Miles, J. W. 1979. On internal solitary waves. *Tellus 31*, 456–462.

Peters, A. S. and Stoker, J. J. 1960. Solitary waves in liquids having non-constant density. *Comm. Pure Appl. Math. 13*, 115–164.

Rayleigh, J. W. S., Lord 1883. The form of standing waves on the surface of running water. *Proc. London Math. Soc. 15*, 69–78.

Temperville, A. 1979. Interaction of solitary waves in shallow water theory. *Archives of Mechanics 31*, 177–184.

Ter-Krikorov, A. M. 1962. On internal waves in an inhomogeneous fluid. *P.P.M. 26*, 1067–1076.

Thorpe, S. A. 1968. On the shape of progressive internal waves. *Phil. Trans. Roy. Soc. A263*, 563–614.

Whitham, G. B. 1974. *Linear and non-linear waves.* New York: Wiley, 636 pp.

Yanowitch, M. 1962. Gravity waves in a heterogeneous incompressible fluid. *Comm. Pure Appl. Math. 15*, 45–61.

ВНУТРЕННИЕ ВОЛНЫ В МЕЛКОЙ ВОДЕ: ТЕОРЕТИЧЕСКОЕ И ЭКСПЕРИМЕНТАЛЬ НОЕ ИССЛЕДОВАНИЕ

С помощью теории мелкой воды исследуются нелинейные внутренние волны в идеальной жидкости в приближении потенциальности движения. После установления общей системы уравнений более полно исследуется частный случай распространяющихся и стоячих волн, что ведет к приближению Буссинеска в приближении первого порядка. В обоих случаях найдено решение в виде кноидальной волны. Для проверки аналитического решения для стоячей внутренней волны проведены лабораторные эксперименты, которые показали, что даже для сильно нелинейных волн наше решение первого приближения описывает форму волны с точностью лучше 5%.